Extracellular Vesicle Isolation Methods Identify Distinct HIV-1 Particles Released from Chronically Infected T-cells.

Sebastian M. Molnar[1,2,3]ł, Yuriy Kim[3]ł, Lindsay Wieczorek[1,2], Anastasia Williams[3], Kajal Ashok Patil[3], Pooja Khatkar[3], Mark F. Santos[4], Gifty Mensah[3], Aurelio Lorico[4], Victoria R. Polonis[1^], Fatah Kashanchi[3^*]

[1]*Military HIV-1 Research Program, Walter Reed Army Institute of Research, Silver Spring, Maryland, USA;* [2]*Henry M. Jackson Foundation for the Advancement of Military Medicine, Bethesda, Maryland USA;* [3]*Laboartory of Molecular Virology, School of System Biology, George Mason University, Manassas, Virginia, USA;* [4]*College of Medicine, Touro University Nevada, Henderson, Nevada, USA.*

ł Both authors contributed equally

^ These senior authors contributed equally

* Correspondence: Fatah Kashanchi, Ph.D., Laboratory of Molecular Virology, George Mason University, Discovery Hall Room 182, 10900 University Blvd., Manassas, VA 20110, USA, Tel.: 703-993-9160, Fax: 703-993-7022, Email: fkashanc@gmu.edu;

KEYWORDS: HIV-1, extracellular vesicles, extracellular particles, exomeres, exosomes, amphisomes, NRTIs, cART, $_{sm}$HIV-1

Supplemental Data:

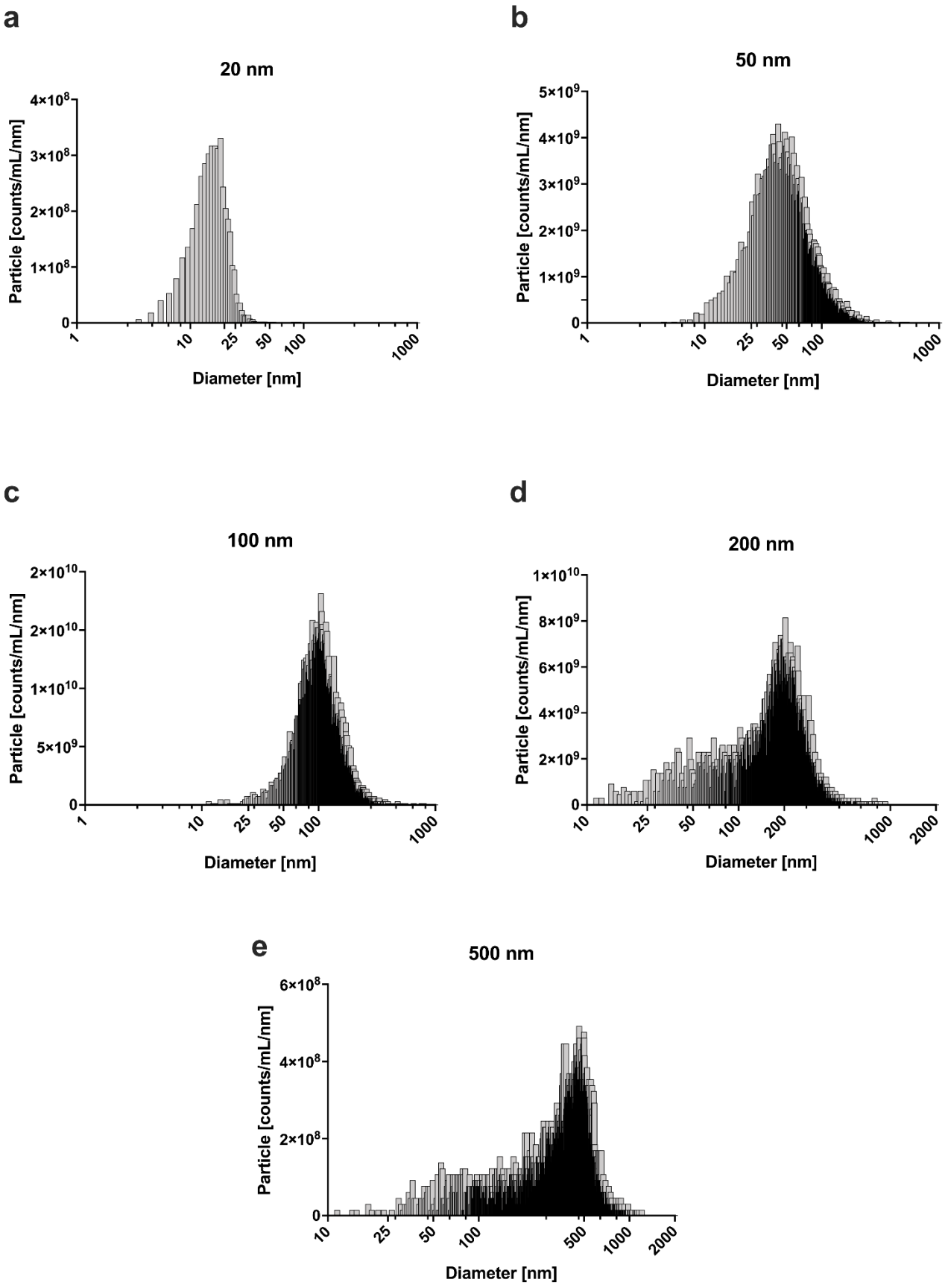
a
20 nm
Particle [counts/mL/nm]
4×10^8
3×10^8
2×10^8
1×10^8
0
1
10
25
50
100
1000
Diameter [nm]
b
50 nm
Particle [counts/mL/nm]
5×10^9
4×10^9
3×10^9
2×10^9
1×10^9
0
1
10
25
50
100
1000
Diameter [nm]
c
100 nm
Particle [counts/mL/nm]
2×10^10
2×10^10
1×10^10
5×10^9
0
1
10
25
50
100
1000
Diameter [nm]
d
200 nm
Particle [counts/mL/nm]
1×10^10
8×10^9
6×10^9
4×10^9
2×10^9
0
10
25
50
100
200
1000
2000
Diameter [nm]
e
500 nm
Particle [counts/mL/nm]
6×10^8
4×10^8
2×10^8
0
10
25
50
100
500
1000
2000
Diameter [nm]

Figure S1: Graphical illustration for the particle size distribution (PSD) of commercially available NanoXact silica standard nanospheres from nanoComposix. a) 20 nm nanosphere product number SISN20; b) 50 nm nanosphere product number SISN50; c) 100 nm nanosphere product number SISN100; d) 200 nm nanosphere product number SISN200; e) 500 nm nanosphere product number SISN500;

NanoXact Silica Nanosphere PSD

Nanosphere (nm)	D10 (nm)	D50 (nm)	D90 (nm)	Mean (nm)	Mode (nm)	SD (nm)	Total Concentration Particles/ml	Product Number
20	9.70	16.38	23.90	17.48	18.60	12	4.25E09	**SISN20**
50	42.45	58.36	124.13	69.34	42.45	45	2.66E11	**SISN50**
100	69.48	104.49	189.54	124.09	104.46	54	1.44E12	**SISN100**
200	88.28	204.30	309.54	206.44	203.54	91	1.10E12	**SISN200**
500	191.70	456.71	614.38	435.95	469.48	166	1.14E11	**SISN500**

Table S1: Nanoparticle tracking analysis (NTA) with particle size distribution (PSD) and total particle concentration per milliliter for commercially available NanoXact silica standard nanospheres from nanoComposix. Data was generated from 50 videos (300 frames/video) processed with “Constant Bins table” with 1nm bin sizes set to integration range between 0-2000 nm. Where D10 is defined as the size distribution where 10% of the sample is contained, D50 is defined as the size distribution where 50% of the sample is contained (median), and D90 is defined as the size distribution where 90% of the sample is contained. SD standard deviation.

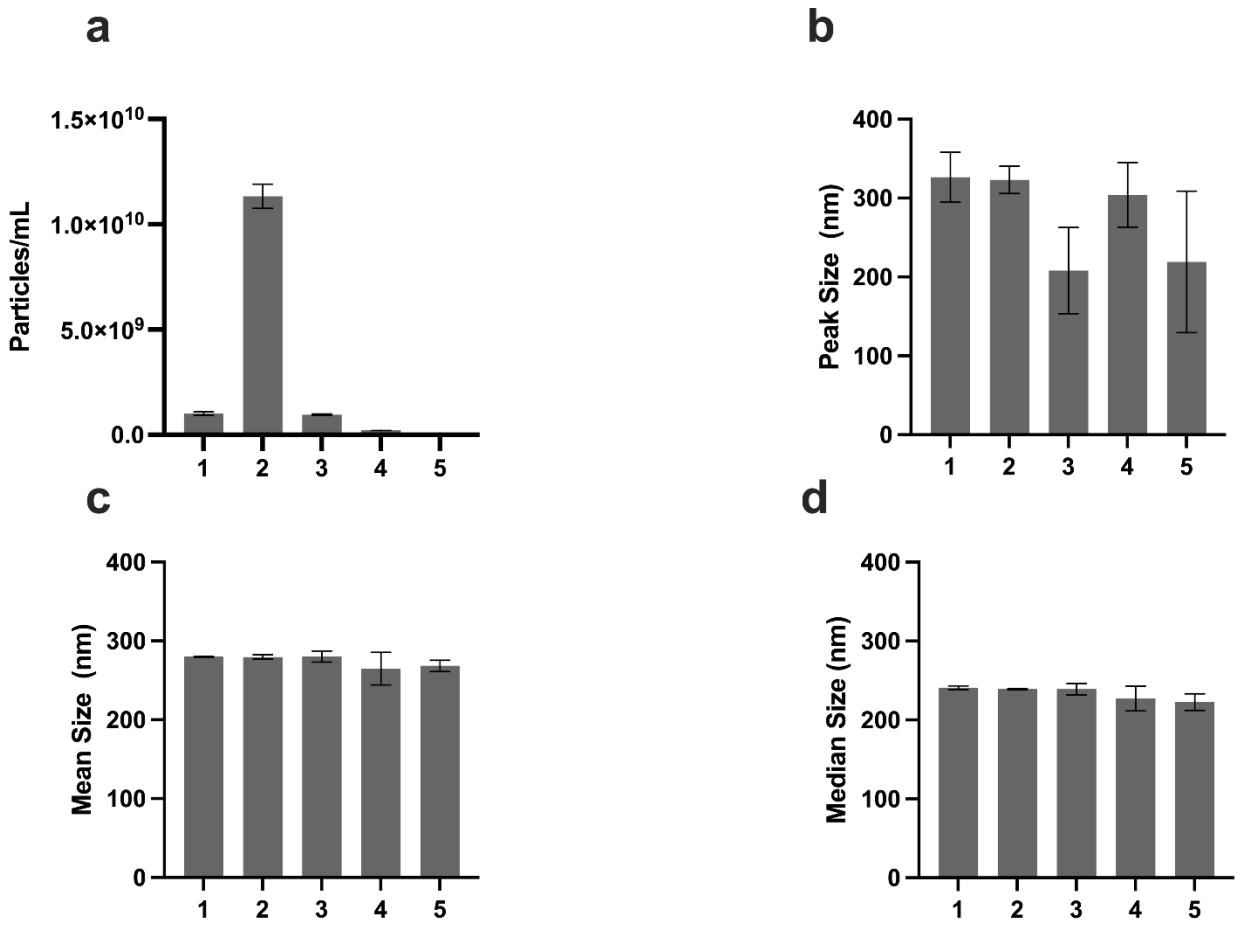

Figure S2: Physical characterization of Frac-A recovered from HIV-1-infected T-cells. J1.1$_{LAV}$ cells (5×10^7) were cultured for five days. Cells were pelleted, and supernatant was centrifuged at 2,000 x g for 45 minutes and fractionated by qEV 70 exclusion column and fractions 1-5 were characterized by NTA analysis to determine (a) EPs concentration, (b) median size, (c) mean size, and (d) peak size. Each bar represents an average of three independent replicates.

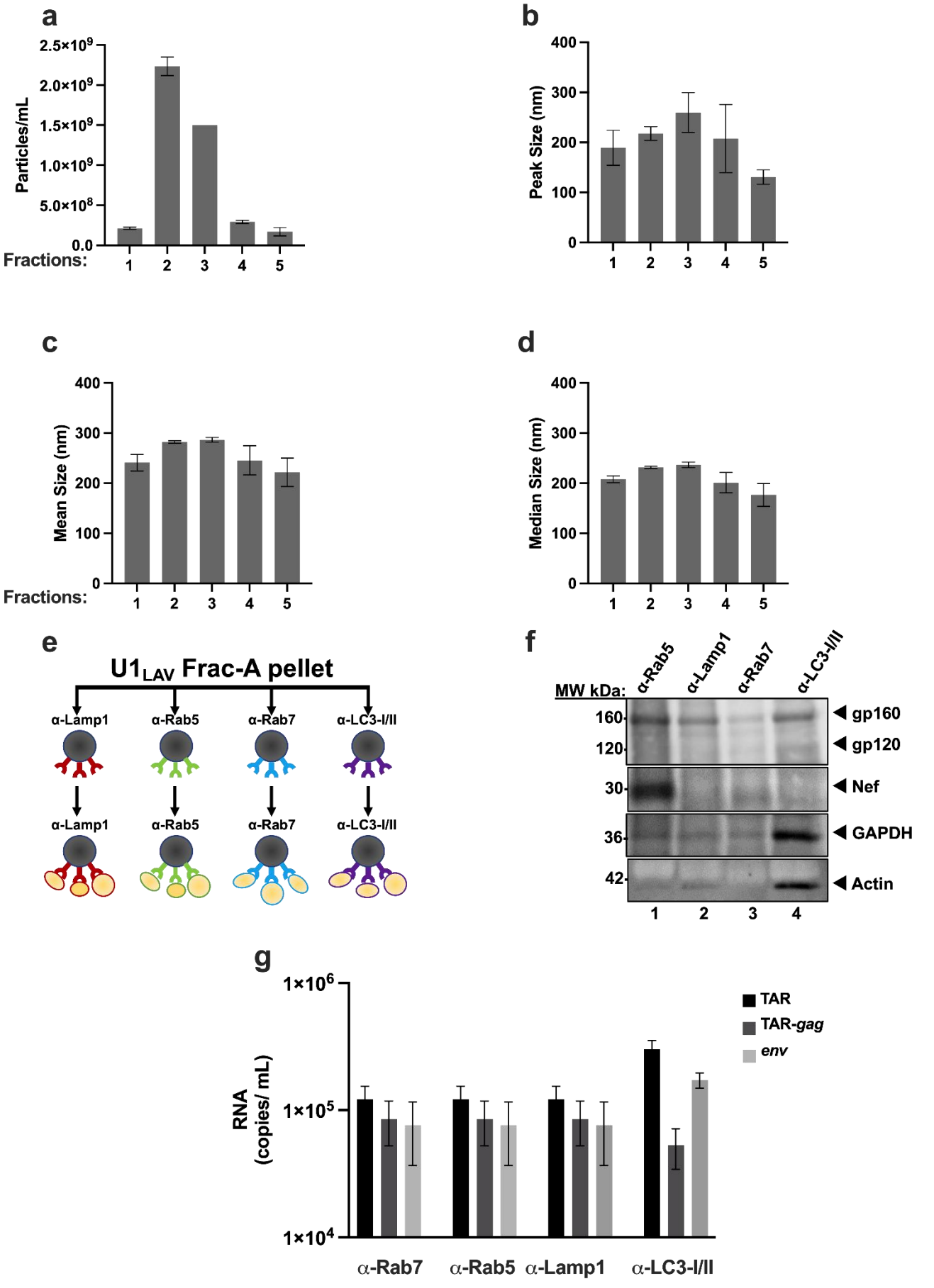
a
Particles/mL
2.5×10^9
2.0×10^9
1.5×10^9
1.0×10^9
5.0×10^8
0.0
Fractions:
1 2 3 4 5
b
Peak Size (nm)
400
300
200
100
0
1 2 3 4 5
c
Mean Size (nm)
400
300
200
100
0
Fractions:
1 2 3 4 5
d
Median Size (nm)
400
300
200
100
0
1 2 3 4 5
e
U1LAV Frac-A pellet
α-Lamp1
α-Rab5
α-Rab7
α-LC3-I/II
α-Lamp1
α-Rab5
α-Rab7
α-LC3-I/II
f
MW kDa:
α-Rab5
α-Lamp1
α-Rab7
α-LC3-I/II
160
120
30
36
42
gp160
gp120
Nef
GAPDH
Actin
1 2 3 4
g
RNA (copies/ mL)
1×10^6
1×10^5
1×10^4
TAR
TAR-gag
env
α-Rab7
α-Rab5
α-Lamp1
α-LC3-I/II

Figure S3: Physical characterization and immunoprecipitation of large EPs fractions from HIV-1-infected monocytes. U1 cells (1×10^8) were cultured for five days. Cells were pelleted, and supernatant was centrifuged at 2,000 x g for 45 minutes and fractionated by qEV 70 exclusion column and fractions 1-5 were characterized by NTA analysis to determine (a) EPs concentration, (b) median size, (c) mean size, and (d) peak size. Each bar represents an average of three independent replicates. Immunoprecipitation (IP) of large EPs from HIV-1-infected monocytes. (e) Principle of immunoprecipitation of Frac-A particles from U1 cells by Lamp1, Rab5, Rab7 and LC3 antibodies. (f) IP-ed samples were pulled down and tested for the presence of viral proteins gp120/160, Nef and viral RNAs (g) such as TAR, TAR-*gag* and *env*.

$J1.1_{LAV}$ and $J1.1_{LAV}$ (NRTIs+) EVPs
Total Particle Count to Total Protein Ratio

	$J1.1_{LAV}$			$J1.1_{LAV}$ (NRTIs+)		
Fractions	Particles/ml Concentration	Total Protein (μg/ml)	Particles/Total Protein	Particles/ml Concentration	Total Protein (μg/ml)	Particles/Total Protein
A	1.50E+10	540	2.78E+07	1.84E+10	561	3.28E+07
B	4.06E+09	4	**1.14E+09**	2.72E+09	33	8.24E+07
C	2.20E+10	113	**1.95E+08**	2.66E+10	14	**1.91E+09**
D	1.70E+10	8	**2.14E+09**	2.37E+10	18	**1.29E+09**
E	5.30E+10	908	5.84E+07	4.73E+10	3952	1.20E+07

Table S2: Particle concentration to total protein ratio of EPs recovered from $J1.1_{LAV}$ naive and $J1.1_{LAV}$ (NRTIs+) treated cell culture. A ration of particle to total protein $>10^8$ indicates acceptable EPs purity (bold numbers), and lower ratios than $<10^8$ indicate the presence of a higher non-EV protein contaminant.

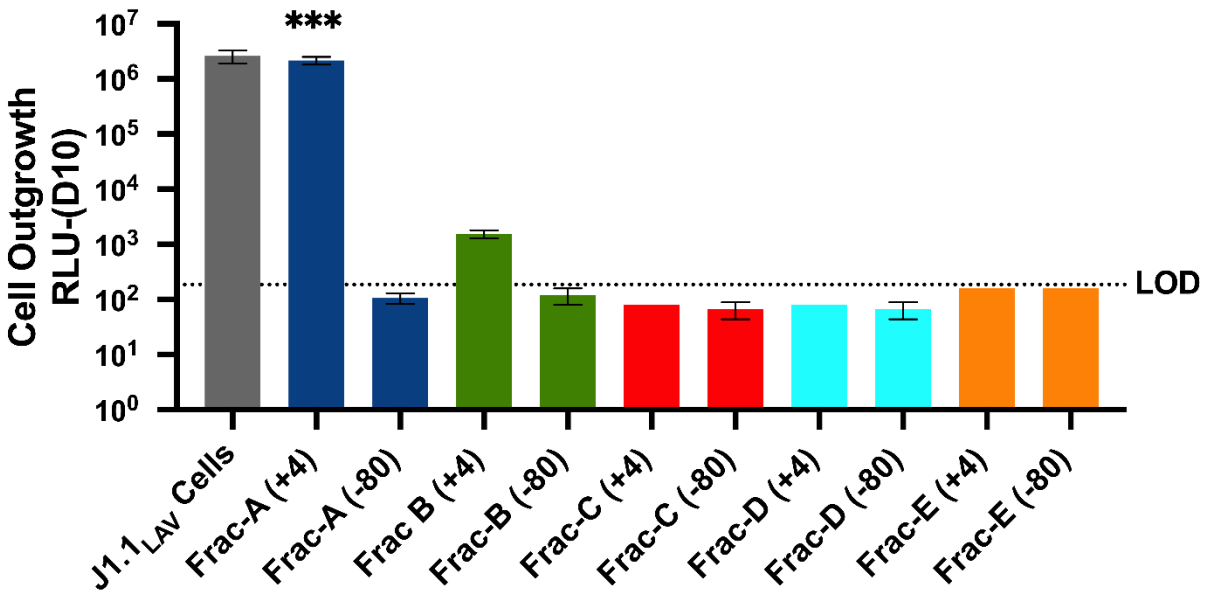

Figure S4: J1.1$_{LAV}$ EPs cell outgrowth assay. The cell outgrowth assay was executed in technical triplicate wells with 25µl of each fraction either stored at +4 ^{o}C or -80 ^{o}C overnight then resuspended in 225µl of culture medium and incubated for ten days. Statistical significance was calculated with One-way ANOVA with Tukey's post-hoc analysis multiple comparisons test with ***: $P < 0.001$ significance level, (LOD) Limit of Detection (3.5 pg/mL)

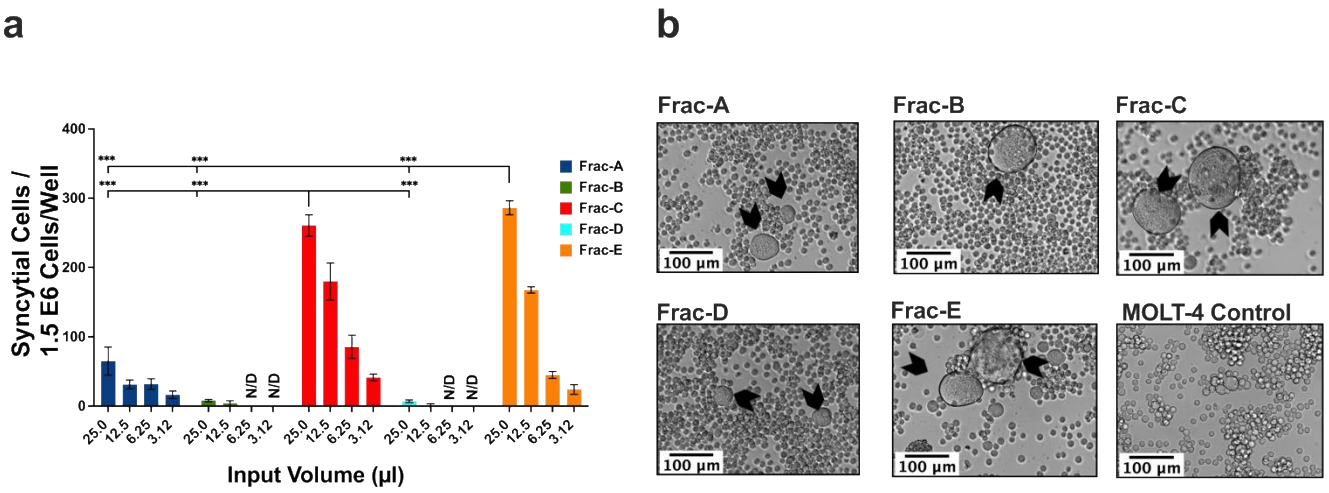

Figure S5: Virus recovery assay (VRA) of J1.1$_{LAV}$ EPs cytopathic effects of Fractions A through E: a) Syncytial cell counts reflecting cytopathic effects of day four MOLT-4 VRA target cells, (N/D) not detected; (b) Micrographs of syncytial cell cytopathic effects observed on MOLT-4 VRA at day four post EPs inputs, black arrows indicated the syncytial cells observed under a 20X magnification in phase-contrast. Data represents mean ± standard deviation (SD) of three technical replicate measurements. Statistical significance was calculated with One-way ANOVA with Tukey's post-hoc analysis multiple comparisons test with *: P < 0.05, **: P < 0.01 ***: P < 0.001, ****: P < 0.0001 significance level. Micrographs were captured with a phase-contrast microscope at 20X magnification with a scale bar representing 100 µm.

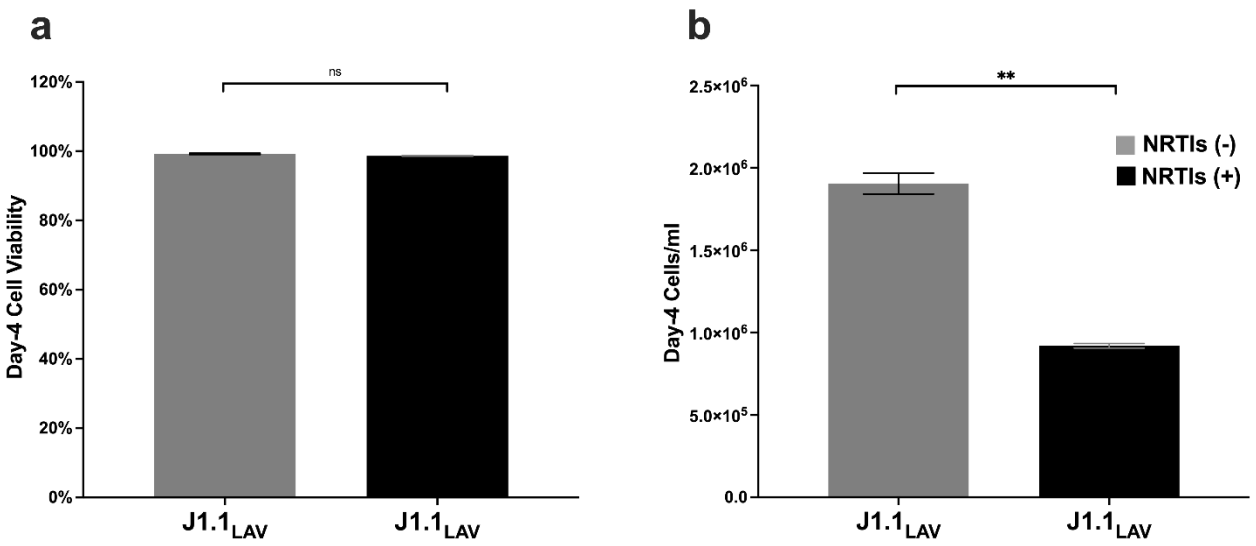

Figure S6: Day four cell growth and viabilities for either J1.1$_{LAV}$ NRTIs naïve or NRTIs treated cell cultures. (a) Cell counts/ml; (b) Cell viabilities for J1.1$_{LAV}$. Statistical significance was calculated with unpaired two-tailed Student's t-test **: $P < 0.02$ significance level obtained from three technical replicate cell counts.

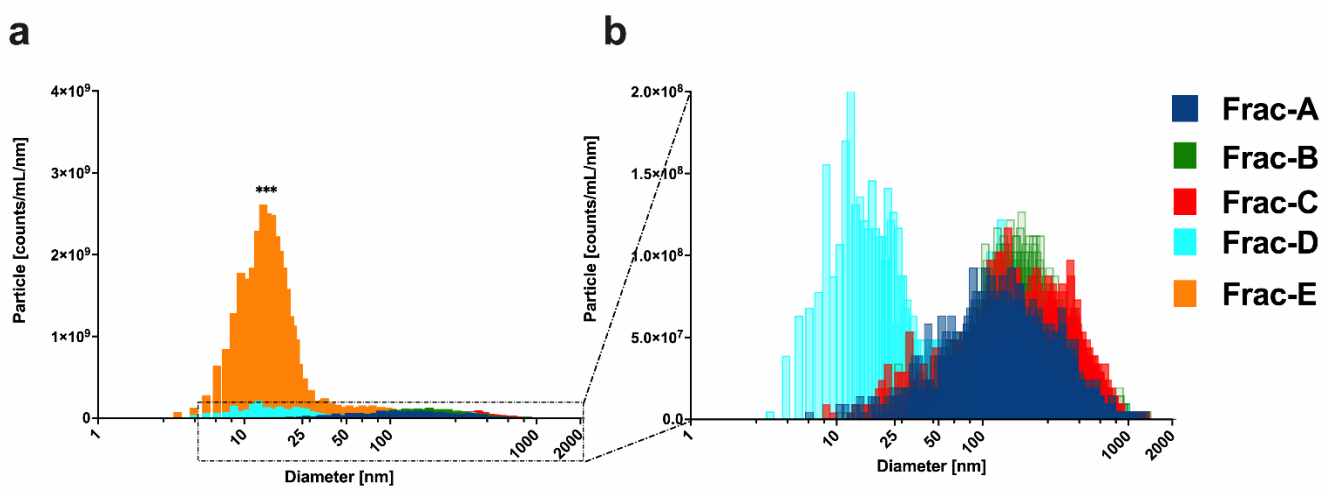

Figure S7: Biophysical characterization NRTI treated J1.1$_{LAV}$ EPs fractions by nanoparticle tracking analysis (NTA). (a) Graphical illustration of the particle size distribution (PSD) for J1.1$_{LAV}$ fractions with Frac-E in comparison to all the other fractions; (b) boxed in section from panel (a) is the magnification PSD for Frac-A through Frac-D. Statistical significance was calculated with One-way ANOVA with Tukey's post-hoc analysis multiple comparisons test with ***: $P < 0.001$ significance level.

J1.1$_{LAV}$ (NRTIs +) EPs PSD

Fractions	D10 (nm)	D50 (nm)	D90 (nm)	Mean (nm)	Mode (nm)	SD (nm)	Total Concentration Particles/ml
A	78	212	484	234	N/A	168	1.84E+10
B	104	236	530	152	186	178	2.72E+09
C	104	296	570	273	150	184	2.66E+10
D	23	201	481	219	13	178	2.37E+10
E	19	17	139	50	14	74	4.73E+10

Table S3: ViewSizer 3000 NTA of each (NRTIs +) J1.1$_{LAV}$ EPs fractions particle size distribution (PSD) with particle size means, mode, standard deviation (SD) and particle concentration (particles/ml). PSD is defined by D10, D50, and D90, where the D10 is the point in the size distribution where 10% of the sample is contained, D50 is the point where 50% of the sample is included (median), and D90 is the point where 90% of the sample is contained. Data was generated from 50 videos (300 frames/video) processed with “Constant Bins Table” with 1nm bin sizes set to integration range between 0-2000 nm.

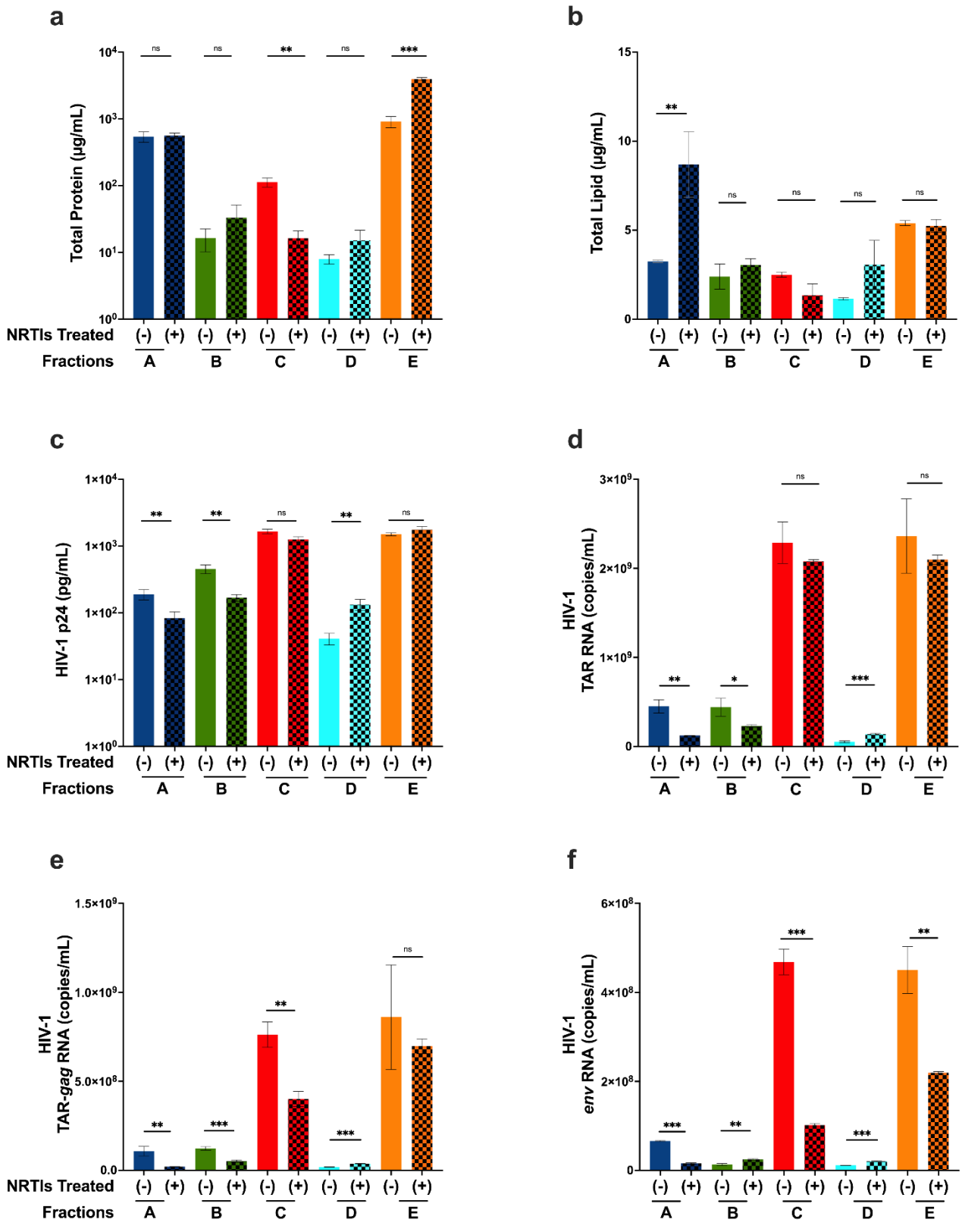
a
Total Protein (µg/mL)
10^4
10^3
10^2
10^1
10^0
ns
ns
**
ns
***
NRTIs Treated
(-) (+) (-) (+) (-) (+) (-) (+) (-) (+)
Fractions
A B C D E
b
Total Lipid (µg/mL)
15
10
5
0
**
ns
ns
ns
ns
(-) (+) (-) (+) (-) (+) (-) (+) (-) (+)
A B C D E
c
HIV-1 p24 (pg/mL)
1×10^4
1×10^3
1×10^2
1×10^1
1×10^0
**
**
ns
**
ns
NRTIs Treated
(-) (+) (-) (+) (-) (+) (-) (+) (-) (+)
Fractions
A B C D E
d
HIV-1
TAR RNA (copies/mL)
3×10^9
2×10^9
1×10^9
0
**
*
ns
***
ns
(-) (+) (-) (+) (-) (+) (-) (+) (-) (+)
A B C D E
e
HIV-1
TAR-gag RNA (copies/mL)
1.5×10^9
1.0×10^9
5.0×10^8
0.0
**
***
**
***
ns
NRTIs Treated
(-) (+) (-) (+) (-) (+) (-) (+) (-) (+)
Fractions
A B C D E
f
HIV-1
env RNA (copies/mL)
6×10^8
4×10^8
2×10^8
0
***
**
***
***
**
(-) (+) (-) (+) (-) (+) (-) (+) (-) (+)
A B C D E

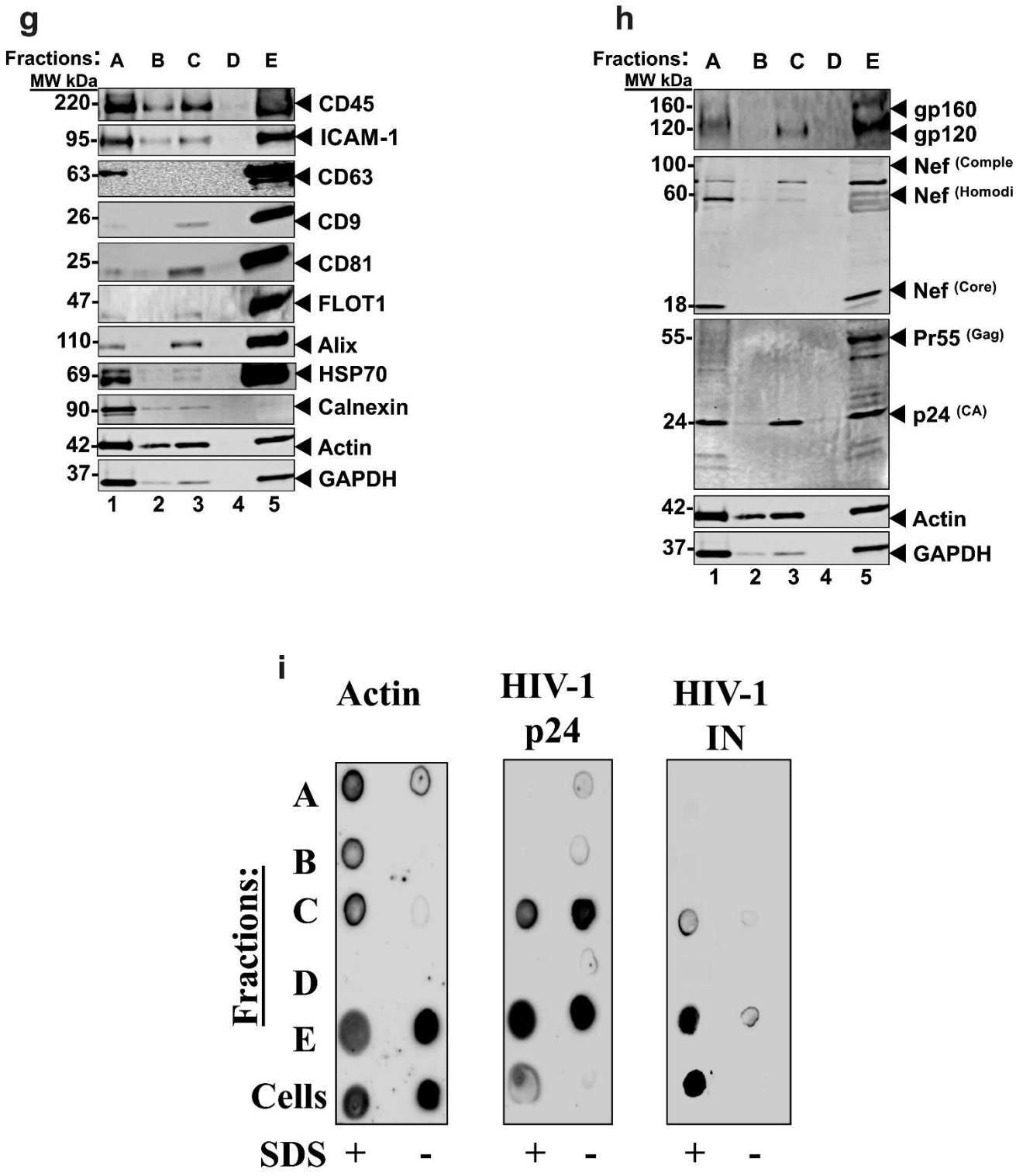
g
Fractions: A B C D E
MW kDa
220-
95-
63-
26-
25-
47-
110-
69-
90-
42-
37-
CD45
ICAM-1
CD63
CD9
CD81
FLOT1
Alix
HSP70
Calnexin
Actin
GAPDH
1 2 3 4 5
h
Fractions: A B C D E
MW kDa
160-
120-
100-
60-
18-
55-
24-
42-
37-
gp160
gp120
Nef (Comple
Nef (Homodi
Nef (Core)
Pr55 (Gag)
p24 (CA)
Actin
GAPDH
1 2 3 4 5
i
Actin
HIV-1 p24
HIV-1 IN
Fractions:
A
B
C
D
E
Cells
SDS + - + - + -

Figure S8: Biochemical content comparison between J1.1$_{LAV}$ EPs recovered from NRTIs naïve or NRTIs treated. (a) Micro BCA total protein content (µg/ml); (b) total lipid assay (µg/ml); (c) HIV-1 p24 antigen capture ELISA (pg/ml); (d) RT-qPCR for non-coding short HIV-1 TAR RNA (copies/ml); (e) RT-qPCR for non-coding HIV-1 TAR-*gag* RNA (copies/ml). (f) RT-qPCR for near full-length HIV-1 genomic *env* RNA (copies/ml); WB of J1.1$_{LAV}$ EPs fractions recovered from NRTIs treated cell culture probe for T-cell marker (CD45), cell adhesion (ICAM-1), extracellular vesicle tetraspanins markers (CD63, CD9, and CD81), extracellular cargo marker (TSG101, Alix, HSP70, Actin) (g) or for r HIV-1 protein content (gp120, Nef, and p24) (h); (i) SDS membrane protection assay dot blotting of J1.1$_{LAV}$ EPs fractions recovered from NRTIs treated cell culture probed for the presence actin and HIV-1 markers (p24, integrase). For each measurement technical triplicates were executed. Statistical significance was calculated with unpaired two-tailed Student's t-test with *: $P < 0.033$; **: $P < 0.02$ ***: $P < 0.001$ significance level for panels (a-f), and with One-way ANOVA with Tukey's post-hoc analysis multiple comparisons test with *: $P < 0.05$, **: $P < 0.01$ ***: $P < 0.001$, ****: $P < 0.0001$ significance level for panel (g).

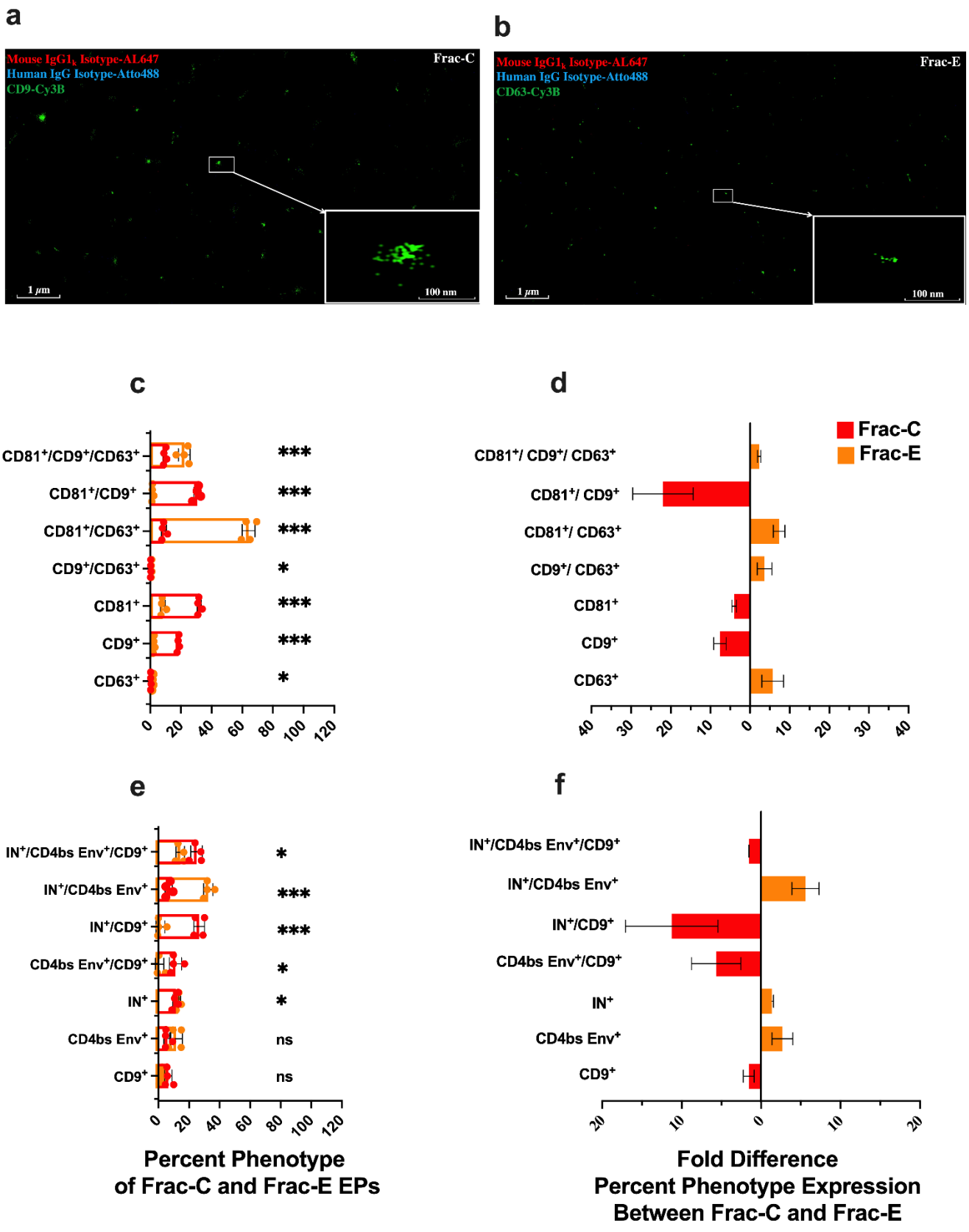
a
Mouse IgG1κ Isotype-AL647
Human IgG Isotype-Atto488
CD9-Cy3B
Frac-C
1 μm
100 nm
b
Mouse IgG1κ Isotype-AL647
Human IgG Isotype-Atto488
CD63-Cy3B
Frac-E
1 μm
100 nm
c
CD81+/CD9+/CD63+
CD81+/CD9+
CD81+/CD63+
CD9+/CD63+
CD81+
CD9+
CD63+
***
***
***
*
***
***
*
0 20 40 60 80 100 120
d
Frac-C
Frac-E
CD81+/ CD9+/ CD63+
CD81+/ CD9+
CD81+/ CD63+
CD9+/ CD63+
CD81+
CD9+
CD63+
40 30 20 10 0 10 20 30 40
e
IN+/CD4bs Env+/CD9+
IN+/CD4bs Env+
IN+/CD9+
CD4bs Env+/CD9+
IN+
CD4bs Env+
CD9+
*
***
***
*
*
ns
ns
0 20 40 60 80 100 120
Percent Phenotype
of Frac-C and Frac-E EPs
f
IN+/CD4bs Env+/CD9+
IN+/CD4bs Env+
IN+/CD9+
CD4bs Env+/CD9+
IN+
CD4bs Env+
CD9+
20 10 0 10 20
Fold Difference
Percent Phenotype Expression
Between Frac-C and Frac-E

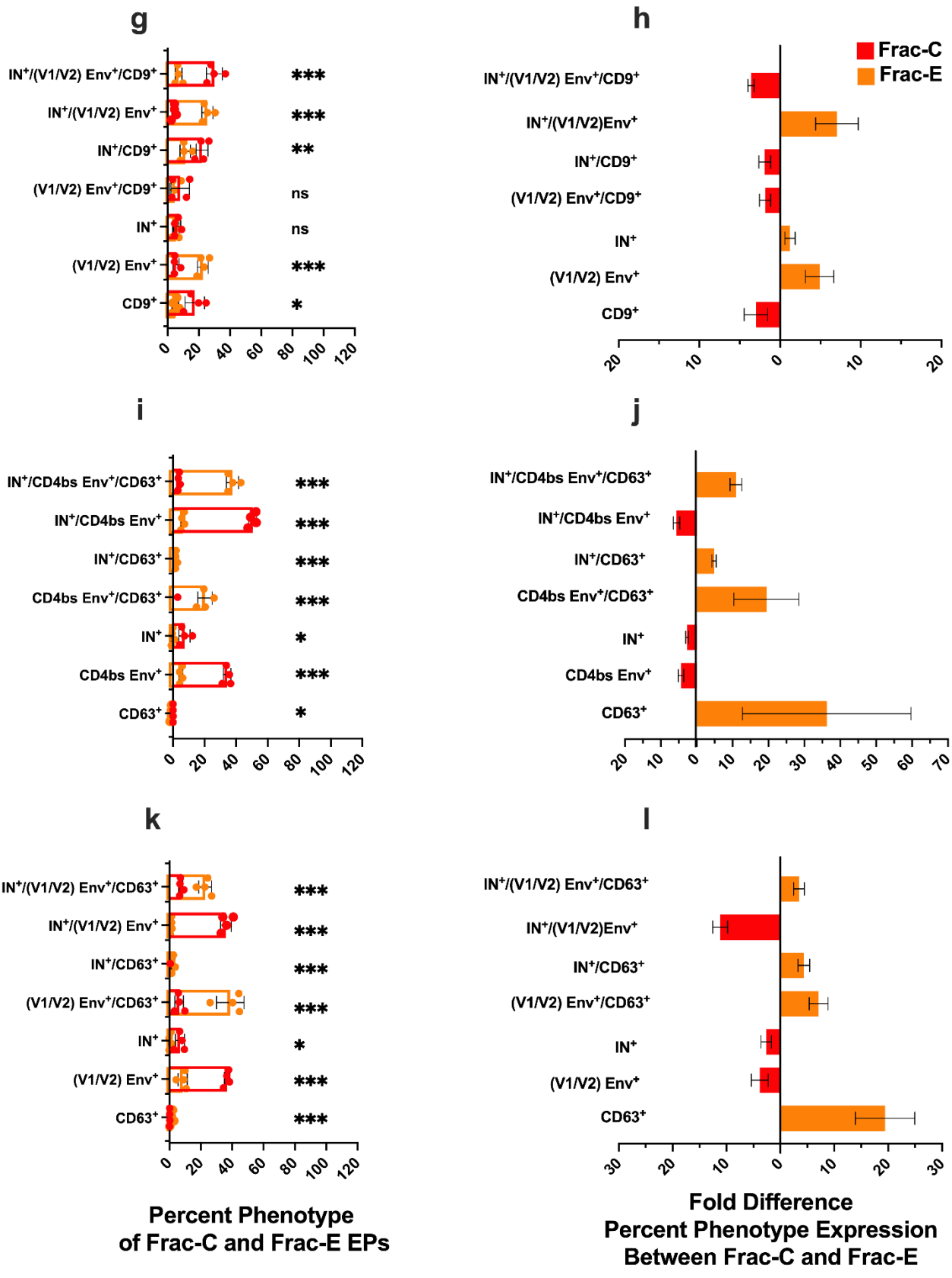
g
IN+/(V1/V2) Env+/CD9+
IN+/(V1/V2) Env+
IN+/CD9+
(V1/V2) Env+/CD9+
IN+
(V1/V2) Env+
CD9+
***
***
**
ns
ns
***
*
0 20 40 60 80 100 120
h
Frac-C
Frac-E
IN+/(V1/V2) Env+/CD9+
IN+/(V1/V2)Env+
IN+/CD9+
(V1/V2) Env+/CD9+
IN+
(V1/V2) Env+
CD9+
20 10 0 10 20
i
IN+/CD4bs Env+/CD63+
IN+/CD4bs Env+
IN+/CD63+
CD4bs Env+/CD63+
IN+
CD4bs Env+
CD63+
***
***
***
***
*
***
*
0 20 40 60 80 100 120
j
IN+/CD4bs Env+/CD63+
IN+/CD4bs Env+
IN+/CD63+
CD4bs Env+/CD63+
IN+
CD4bs Env+
CD63+
20 10 0 10 20 30 40 50 60 70
k
IN+/(V1/V2) Env+/CD63+
IN+/(V1/V2) Env+
IN+/CD63+
(V1/V2) Env+/CD63+
IN+
(V1/V2) Env+
CD63+
***
***
***
***
*
***
***
0 20 40 60 80 100 120
Percent Phenotype
of Frac-C and Frac-E EPs
l
IN+/(V1/V2) Env+/CD63+
IN+/(V1/V2)Env+
IN+/CD63+
(V1/V2) Env+/CD63+
IN+
(V1/V2) Env+
CD63+
30 20 10 0 10 20 30
Fold Difference
Percent Phenotype Expression
Between Frac-C and Frac-E

Figure S9: dSTORM images and comparisons analysis between J1.1$_{LAV}$ Frac-C and Frac-E EPs percent phenotype and fold difference percent phenotype expression: (a-b) wide field of view and single particle insert representative dSTROM images of tetraspanin and HIV-1 mAbs isotype control stainings with CD9^{+}/Mouse IgG1$_{k}^{-}$/Human IgG^{-} of Frac-C and CD63^{+}/Mouse IgG1$_{k}^{-}$/Human IgG^{-} of Frac-E EPs; (c-d) tetraspanin phenotype characterization Frac-C and Frac-E; HIV-1 phenotype characterization of Frac-C and Frac-E stained with mAbs against CD9-Cy3B and HIV-1 IN (2C11-AL647) costained either with VRC01-Atto488 gp120 CD4bs specific mAb (e-f) or with PG16-Atto488 gp120 V1/V2 specific mAb (g-h); HIV-1 phenotype characterization of Frac-C and Frac-E stained with CD63^{+}-Cy3B and HIV-1 IN (2C11-AL647) costained either with VRC01-Atto488 gp120 CD4bs specific mAb (i-j) or with PG16-Atto488 gp120 V1/V2 specific mAb(k-l). For each measurement technical quadruplicates were executed from a samples size n>5000 EPs. dSTORM images analyzed over (n > 5000 EPs per quadruplicate experiment). Statistical significance for panels (c, e, g, i, and k) was calculated with unpaired two-tailed Student's t-test with *: $P < 0.05$; **: $P < 0.01$ **: $P < 0.001$*** significance.

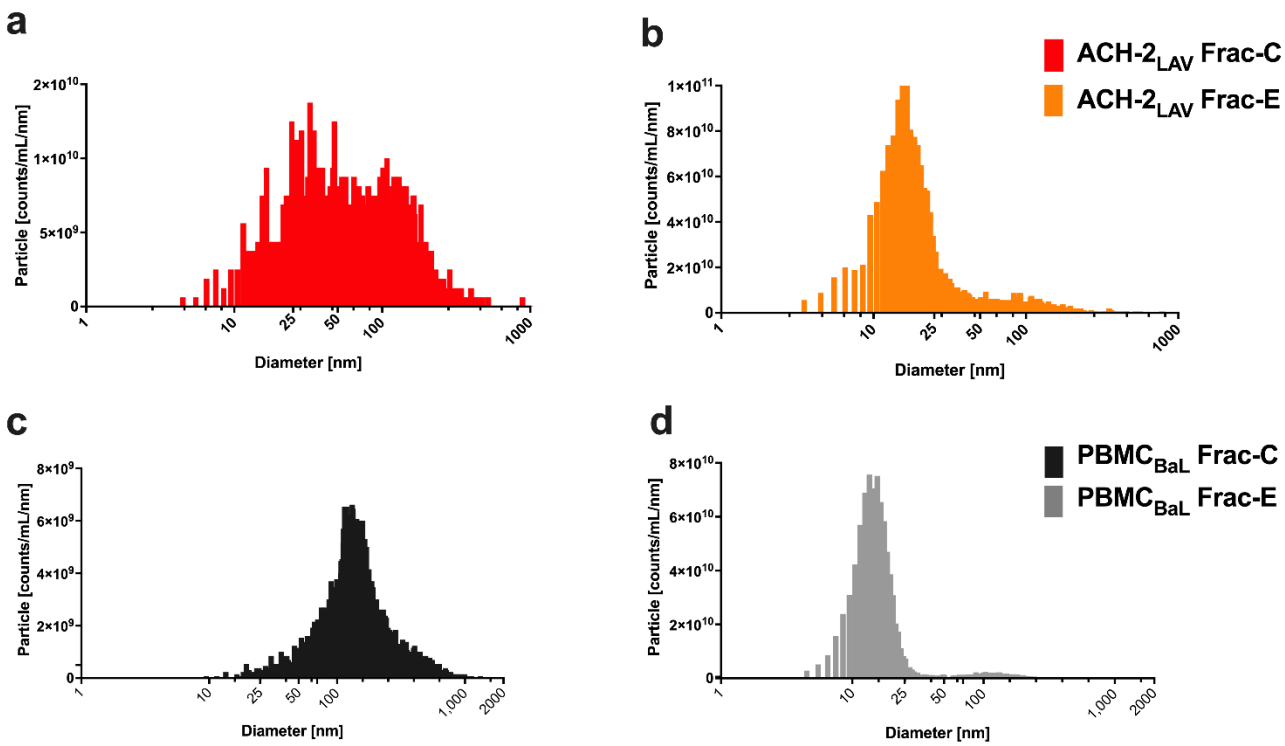

e

PSD of Frac-C and Frac-E EPs Derived from ACH-2_{LAV} and $PBMC_{BAL}$

Sample	D10 (nm)	D50 (nm)	D90 (nm)	Mean (nm)	Mode (nm)	SD (nm)	Total Concentration Particles/ml
AHC-2_{LAV} Frac-C	32	97	196	107	32	75	1.18E12
$PBMC_{BaL}$ Frac-C	90	166	441	219	131	151	9.17E11
AHC-2_{LAV} Frac-E	11	20	123	47	15	67	1.96E12
$PBMC_{BaL}$ Frac-E	10	16	140	46	14	72	1.04E12

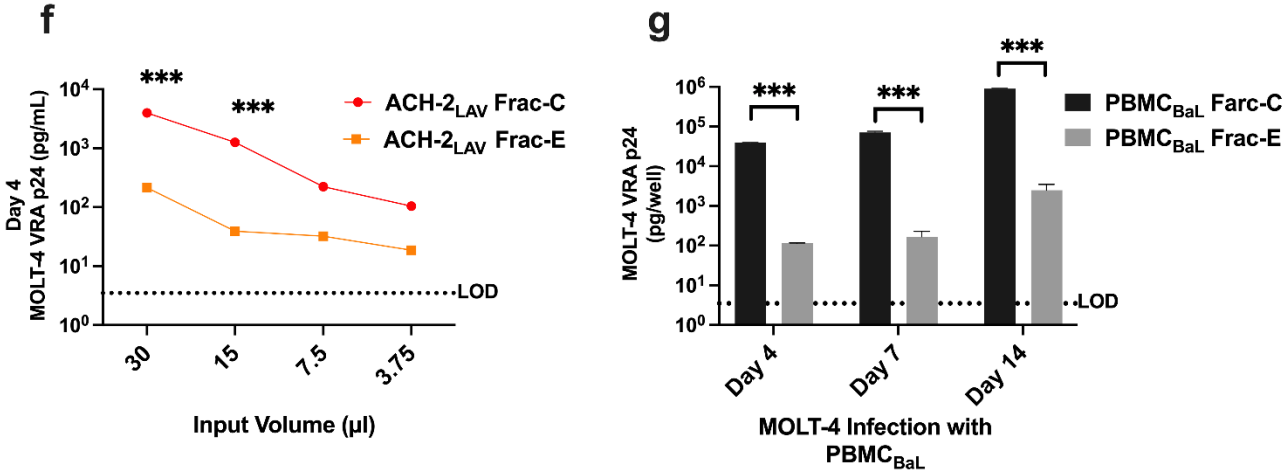

Figure S10: Biophysical and functional characterization of ACH-2_{LAV} Frac-C/Frac-E and HIV-1 BaL infected PBMCs ($PBMC_{BaL}$) **Frac-C/Frac-E EPs.** NTA graphical illustration of the particle size distribution (PSD) for Frac-C and Frac-E (a-b) ACH-2_{LAV} and $PBMC_{BaL}$ Frac-C and Frac-E (c-d); (c) tabulated particle size distribution (PSD) for EPs derived from ACH-2_{LAV} and $PBMC_{BaL}$, with particle size distribution D10, D50 D90, means, mode, standard deviation (SD) and particle concentration (particles/ml); (f) ACH-2_{LAV} Frac-C and Frac-E MOLT-4 VRA supernatant p24 capture ELISA pg/mL levels measured on day four; (g) $PBMC_{BaL}$ Frac-C and Frac-E MOLT-4 VRA supernatant p24 capture ELISA pg/mL levels measured on days four seven and fourteen. PSD of D10, D50, and D90, is defined as where the D10 is the point in the size distribution where 10% of the sample is contained, D50 is the point where 50% of the sample is included (median), and D90 is the point where 90% of the sample is contained. Data was generated from 50 videos (300 frames/video) processed with “Constant Bins Table” with 1nm bin sizes set to integration range between 0-2000 nm. Data for the viral p24 capture ELISA represents mean ± standard deviation (SD) of three technical replicate measurements, (LOD) Limit of Detection (3.5 pg/mL). Statistical significance was calculated with One-way ANOVA with Tukey’s post-hoc analysis multiple comparisons test with ***: $P < 0.001$, significance level.

a

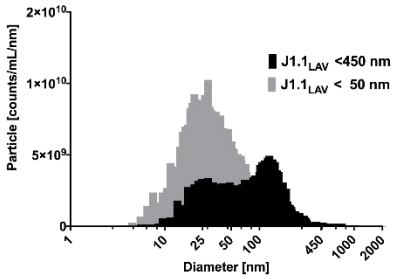

b

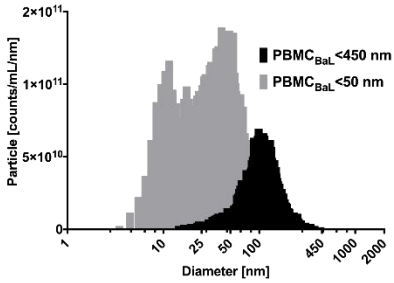

c

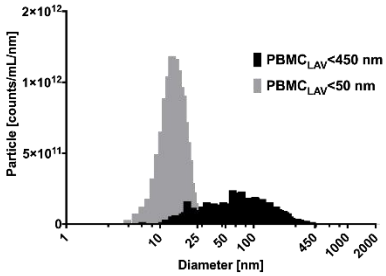

d

PSD for 450 nm and 50 Differentially Filtered EPs Derived from $J.1.1_{LAV}$, PBMC Infected with BaL and LAV

Sample	D10 (nm)	D50 (nm)	D90 (nm)	Mean (nm)	Mode (nm)	SD (nm)	Total Concentration Particles/ml
$J1.1_{LAV}$ <450 nm	36	123	232	135	127	96	6.37E11
$PBMC_{BaL}$ <450 nm	68	119	201	130	98	65	6.22E12
$PBMC_{LAV}$ <450 nm	38	108	225	124	59	81	2.43E11
$J1.1_{LAV}$ <50 nm	18	48	132	47	28	58	5.59E11
$PBMC_{BaL}$ <50 nm	14	44	78	46	14	35	7.70E12
$PBMC_{LAV}$ <50 nm	10	16	55	24	13	30	1.46E13

e $J1.1_{LAV}$<450 nm

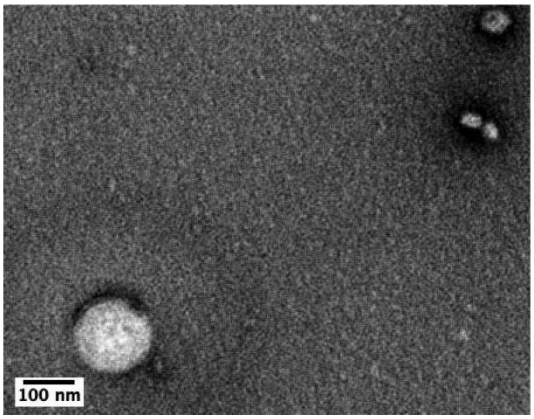

f $J1.1_{LAV}$<50 nm

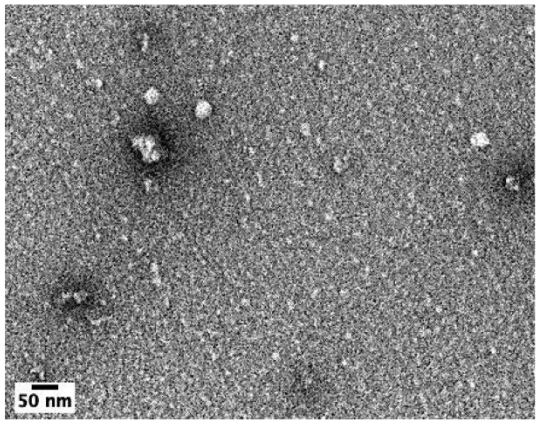

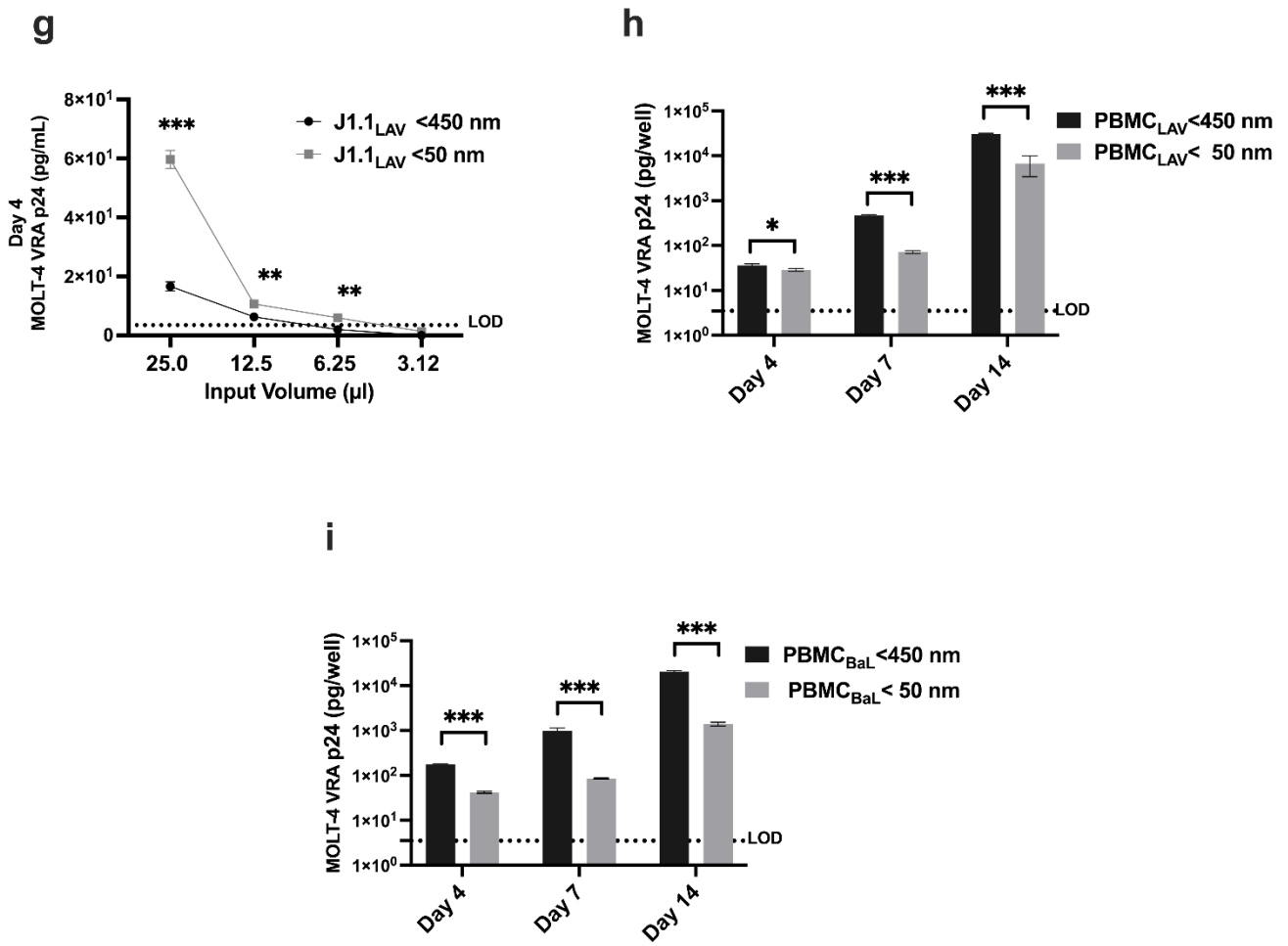

Figure S11: Alternative isolation method of small size EPs recovered from J1.1$_{LAV}$ and HIV-1 infected PBMCs with BaL and LAV virus stocks (PBMC$_{BaL}$ and PBMC$_{LAV}$) with biophysical and functional characterization. (a) diagram of sequential filtration steps with endpoint assays; graphical illustration of the NTA (PSD) for the <450 nm and <50 nm EPs recovered from the retentate of J1.1$_{LAV}$ (b), PBMC$_{BaL}$ (c) respectively PBMC$_{LAV}$ (d); (e) tabulated results for NTA PSD with D10, D50, and D90, mean, mode standard deviation (SD) and total concentration of particles/ mL, for <450 nm and <50 nm EPs J1.1$_{LAV}$, PBMC$_{Bal}$, PBMC$_{LAV}$ retentate; (f) and (g) TEM representative micrographs of <450 nm and <50 nm J1.1$_{LAV}$ EPs retentate; (h) viral p24 capture ELISA of day four MOLT-4 VRA assay of J1.1$_{LAV}$ EPs retentate <450 and <50 retentate; (i-j) p24 capture ELISA of day four, seven, and fourteen of MOLT-4 VRA assay infected culture supernatant with <450 and <50 retentates of PBMC$_{LAV}$ (i) and PBMC$_{BaL}$ (j). The PSD D10 is defined as the is the point in the PSD where 10% of the sample is contained, D50 is the point where 50% of the sample is included (median), and D90 is the point where 90% of the sample is contained additionally. The data for the PSD was generated from 50 videos (300 frames/video) processed with “Constant Bins Table” with 1nm bin sizes set to integration range between 0-2000 nm. The MOLT-4 VRA p24 capture ELISA was executed as technical triplicate measurements, (LOD) lower limit of detection (3.5 pg/mL). Statistical significance for panels (b, i, j) was calculated with unpaired two-tailed Student’s t-test according to its distribution where the *: $P < 0.022$ ***: $P < 0.001$ significance and for panel (h) was calculated with One-way ANOVA with Tukey’s post-hoc analysis multiple comparisons test with **: $P < 0.01$ ***: $P < 0.001$, significance level. Scale bars on the electron micrograph images represent 100 nm and 50 nm.